

# Accepted Manuscript

## Regular Article

### Protective Composite Silica/Polyelectrolyte Shell with Enhanced Tolerance to Harsh Acid and Alkali Conditions

Hui Gao, Thaaqib Nazar, Zhongliang Hu, Dongsheng Wen, Gleb B. Sukhorukov

PII: S0021-9797(17)31197-9  
DOI: <https://doi.org/10.1016/j.jcis.2017.10.038>  
Reference: YJCIS 22908

To appear in: *Journal of Colloid and Interface Science*

Received Date: 29 August 2017  
Revised Date: 9 October 2017  
Accepted Date: 10 October 2017

Please cite this article as: H. Gao, T. Nazar, Z. Hu, D. Wen, G.B. Sukhorukov, Protective Composite Silica/Polyelectrolyte Shell with Enhanced Tolerance to Harsh Acid and Alkali Conditions, *Journal of Colloid and Interface Science* (2017), doi: <https://doi.org/10.1016/j.jcis.2017.10.038>

This is a PDF file of an unedited manuscript that has been accepted for publication. As a service to our customers we are providing this early version of the manuscript. The manuscript will undergo copyediting, typesetting, and review of the resulting proof before it is published in its final form. Please note that during the production process errors may be discovered which could affect the content, and all legal disclaimers that apply to the journal pertain.



# Protective Composite Silica/Polyelectrolyte Shell with Enhanced Tolerance to Harsh Acid and Alkali Conditions

Hui Gao,<sup>\*,†,‡</sup> Thaaqib Nazar,<sup>†</sup> Zhongliang Hu,<sup>‡</sup> Dongsheng Wen,<sup>‡,§</sup> Gleb B. Sukhorukov<sup>\*,†</sup>

<sup>†</sup> School of Engineering and Materials Science, Queen Mary University of London, Mile End Road, London E1 4NS, United Kingdom

<sup>‡</sup> School of Chemical and Processing Engineering, University of Leeds, Leeds LS2 9JT, United Kingdom

<sup>§</sup> School of Aeronautic Science and Engineering, Beihang University, Beijing, 100191, P.R.China

**ABSTRACT:** Here we report a facile method to fabricate composite polymeric/inorganic shells consisting of poly(allylamine hydrochloride) (PAH)/poly-(sodium 4-styrenesulfonate) (PSS) multilayers strengthened by the *in situ* formed silica (SiO<sub>2</sub>) nanoparticles (NPs), achieving an enhanced stability under harsh acidic and basic conditions. While the unsiliconised PAH/PSS multilayers show a pH-dependent stability and permeability, the composite PAH/PSS/SiO<sub>2</sub> shells display significantly higher chemical tolerance towards a variety of harsh conditions ( $1 \leq \text{pH} \leq 13$ , high salinity). Upon treatment with either hydrochloric acid (HCl, pH=1) or 0.2 M ethylenediaminetetraacetic acid disodium salt (EDTA, weak acid, chelator), the (PAH/PSS)<sub>6</sub>/SiO<sub>2</sub> shells are able to maintain the integrity of most calcium carbonate (CaCO<sub>3</sub>) particles, as the shells are tickened and densified by sufficient SiO<sub>2</sub> NPs. When treated with NaOH solution at pH=13, the (PAH/PSS)<sub>6</sub>/SiO<sub>2</sub> shells also display an intact morphology and maintain the ability to intercept rhodamin B (Rh-B) molecules, which is quite different to that observed with the unsiliconised (PAH/PSS)<sub>6</sub> shells. Ultrasound is

proved to rapidly break the composite shells, hence can be used as a potential stimulus to trigger the release of encapsulated substances. All the results demonstrate the fact that the composite (PAH/PSS)<sub>6</sub>/SiO<sub>2</sub> shells have a higher chemical stability, lower permeability for small molecules and a greater sensitivity to ultrasound, which is promising for many applications where protecting the activity of small molecules is required, such as the delivery of encapsulated drugs in an unhindered form to their specific destination within the human body.

**KEYWORDS:** enhanced acid/alkali tolerance, composite shell, *in situ*, SiO<sub>2</sub>, ultrasound responsiveness

## 1. Introduction

Microencapsulation techniques have generated considerable interest to scientists as they can be widely used to protect substances with poor survival and stability under harsh conditions.<sup>[1,2]</sup> For oil/gas recovery applications, improving the stability of surfactants under high salinity or high temperature environments is of great importance to achieving high-yield oil/gas but still presenting as a huge challenge.<sup>[3]</sup> For biological and biomedical applications, chemical stability of pharmaceutical molecules, as well as live bacterial cells for therapeutic purposes such as probiotics, is a matter of great concern as it affects the safety, efficacy and therapeutic effects of the drug products.<sup>[4-6]</sup> Delivering the active ingredients via protective carriers and releasing them at desired locations can significantly reduce the side effects on normal tissues and increase their therapeutic effects. Hence, it has intrigued the researchers to entrap active cargo in a protective shell and thereby keep them intact before being delivered to the target area.<sup>[7-9]</sup>

Porous  $\text{CaCO}_3$  particles have shown good capability in encapsulating micro-molecules such as DNA,<sup>[10]</sup> and siRNA,<sup>[11]</sup> but they are unable to survive under the extreme pH conditions of stomach, which ultimately inhibits their application in oral delivery.<sup>[12,13]</sup> The stomachs of most vertebrates operate at harsh acidic environments, i.e., with pH =2 generated by the gastric  $\text{H}^+/\text{K}^+$ -ATPase located in parietal cells,<sup>[12]</sup> therefore requiring the acid-sensitive payloads to be coated with protective layers able to tolerate such harsh conditions. Similarly, if the payloads are unstable in alkaline conditions, a protective coating with resistance to alkaline solvent is needed. To ensure the chemical stability of the encapsulated materials, developing a type of protective shell with great tolerance to both harsh acidic and alkaline conditions is of great importance. This has the potential to benefit many areas of science from the field of biology to that of energy and the environment.

Various coating materials have been proposed to fabricate protective shells in the past few decades,<sup>[11,14,15]</sup> including polymers and inorganic NPs. Polymeric building blocks such as poly-L-arginine hydrochloride (PARG), dextran sulfate (DEXS), PAH, PSS, etc. can be simply coated on the particles (e.g.,  $\text{CaCO}_3$ ) via the Layer-by-Layer (LbL) method.<sup>[11,16]</sup> These kinds of polymeric multilayers have the advantages of tuneable thickness, good repeatability, variable compositions and functions, and can be used as drug carriers, biosensors, microcontainers, etc..<sup>[16]</sup> However, such polymeric LbL shells often suffer from a few inherent limitations: (i) relatively high sensitivity to environmental fluctuation such as ionic strength, i.e., swelling or shrinking upon changing the pH value of the environment;<sup>[17,18]</sup> (ii) relatively high permeability due to the intrinsic porous structure of polymeric multilayers, which hinders the encapsulation of small molecules<sup>[16,19]</sup> and (iii) relatively weak mechanical strength because of the soft and film-like texture of polymer shells, which tend to collapse under the dry state.<sup>[20]</sup> For example, hollow PAH/PSS capsules are widely studied and show great potential as carriers for drugs, micro-/nano-particles, surfactants, etc.,<sup>[20]</sup> but they are

unstable in harsh alkaline conditions and still struggle with the encapsulation of small molecules.<sup>[17]</sup> Two common methods employed to address those limitations include, increasing the layer number,<sup>[21]</sup> or crosslinking the multilayers either by high temperature treatment,<sup>[16]</sup> UV irradiation,<sup>[22]</sup> chemical reagents,<sup>[23]</sup> or ionization.<sup>[24]</sup> Increasing the layer number may help to some extent, but it brings the difficulty in releasing the cargo due to the electrostatic nature of polyelectrolytes.<sup>[16,25]</sup> The harsh treatment conditions for crosslinking the polymers may damage the pre-loaded molecules, bacterial cells or biological tissues.<sup>[25]</sup> UV irradiation, utilized for polymer crosslinking, is harmful to normal tissues. The UV irradiation on normal human skin may cause sunburn inflammation (erythema), tanning, and local or systemic immunosuppression.<sup>[26]</sup> Moreover, such approaches cannot significantly decrease shell permeability to enable small molecules encapsulation and cannot drastically increase the shell's resistance to high concentration of  $H^+$  or  $OH^-$ .

Introducing rigid inorganic NPs in shells opens up another avenue, and is receiving increasing interest.<sup>[27]</sup> The advantages of inorganic materials, *i.e.* high thermal/chemical stability and resistance to erosion under extreme conditions, are complementary to the soft nature of polymeric shells.<sup>[25]</sup> For example, Wang and Caruso synthesized solid composite microspheres to encapsulate enzymes in mesoporous silica spheres, and demonstrated an enhanced pH stability and recycling stability compared to pure polymeric microcapsules.<sup>[28]</sup> To date, inorganic NPs, such as Au,  $Fe_3O_4$ , ZnO, were commonly introduced individually via a two-step method (*i.e.*, the NPs were prefabricated and then incorporated in polymeric shells),<sup>[16,29,30]</sup> which would strengthen the mechanics of the capsules and increase their sensitivity to external stimuli. However in spite of this the shell permeability could not be significantly decreased. Recently, an *in situ* method was proposed to synthesize and assemble inorganic NPs in polymeric multilayers, which yielded the properties of composite shell much

superior to those constructed via the two-step method.<sup>[16]</sup> For both approaches, however, the effects of inorganic NPs on the shell tolerance to harsh pH conditions are seldom studied.

By introducing the pre-fabricated inorganic NPs, the hybrid polymeric-inorganic shells would not be a continuous and integral shell,<sup>[25]</sup> which has been exemplified by G. B. Sukhorukov et al.<sup>[31,32]</sup> The electrostatic attractive force between the polymeric layers and inorganic NPs is likely to be reduced by the elevated ionic strength, leading to a destruction of the hybrid shell.<sup>[32]</sup> In contrast, the inorganic NPs introduced by the *in situ* synthesis and growth method, act as additional robust building blocks in and around the polymeric multilayers, concrete the multilayer shell and thusly help creating a dense composite shell. As the solid NPs are formed in the free spaces (e.g., pores, concaves, etc.) in the flexible and soft polymer multilayers, they could inhibit the movement of soft polymers. The resistance to extreme pH conditions, as a result, is expected to be significantly improved. Herein the behaviour of polymeric-inorganic composite shells (fabricated by the *in situ* synthesis of inorganic NPs into the polymeric matrix) are investigated in detail. Our earlier study demonstrated that SiO<sub>2</sub> NPs can be formed *in situ* and assembled into the shell of hollow polyelectrolyte microcapsules, producing composite capsules with increased shell thickness, enhanced mechanics and reduced permeability.<sup>[16]</sup> In this work, silica NPs are still chosen as the property enhancer, and PAH/PSS is employed as polymeric building block. Porous CaCO<sub>3</sub> particles and rhodamine-B (Rh-B) are used as the model cargoes that need to be protected. Robust polymeric-inorganic composite shells, i.e. PAH/PSS/SiO<sub>2</sub>, are formed by the *in situ* synthesis of SiO<sub>2</sub> NPs in PAH/PSS shells based on the hydrolysis of tetraethyl orthosilicate (TEOS). For comparison, pure polyelectrolytes shells (PAH/PSS multilayers) and pure inorganic SiO<sub>2</sub> coating fabricated by the same *in situ* process were also produced. The performance of the different shells treated by HCl solution with pH=1 and 0.2 M EDTA solution were then investigated. The

capability of PAH/PSS/SiO<sub>2</sub> microcapsules on encapsulating and releasing small molecules under harsh alkaline environment (NaOH, pH=13) was also explored.

## 2 Experimental Section

**2.1 Materials.** Poly(allylamine hydrochloride) (PAH, Mw = 56 kDa), poly(sodium 4-styrenesulfonate) (PSS, Mw = 70 kDa), Tetraethyl orthosilicate (TEOS, Si(OC<sub>2</sub>H<sub>5</sub>)<sub>4</sub>, ≥ 99.0 %), ammonium hydroxide solution (NH<sub>4</sub>OH, 28.0-30.0% NH<sub>3</sub> basis), dextran-tetramethylrhodamine isothiocyanate (TRITC-dextran, Mw = 500 kDa, ~1 TRITC per 100 glucose residues), rhodamine B (Rh-B, Mw = 479, ≥ 95.0 %), ethylenediaminetetraacetic acid disodium salt (EDTA, ≥ 99.0%), and other salts including calcium chloride (CaCl<sub>2</sub>), sodium carbonate (Na<sub>2</sub>CO<sub>3</sub>), HCl and NaOH were purchased from Sigma-Aldrich.

**2.2 Composite shell preparation.** CaCO<sub>3</sub> microparticles were freshly prepared as reported previously.<sup>[16]</sup> A 0.33 M CaCl<sub>2</sub> solution was mixed under magnetic stirring with the same volume of 0.33 M Na<sub>2</sub>CO<sub>3</sub> solution. After 15 s, the CaCO<sub>3</sub> particles were then collected and washed three times with deionized water (DI-water). TRITC-dextran molecules were encapsulated by coprecipitating them together with the CaCO<sub>3</sub> during the formation process. PAH (positively charged, 2 mg/mL in 0.5 M NaCl) and PSS (negatively charged, 2 mg/mL in 0.5 M NaCl) were then assembled on the CaCO<sub>3</sub> particle via the LbL technique. Different layers of polyelectrolytes (8 and 12 layers) were assembled, to form CaCO<sub>3</sub>/(PAH/PSS)<sub>4</sub> and CaCO<sub>3</sub>/(PAH/PSS)<sub>6</sub> complex particles. Subsequently, these particles were coated with SiO<sub>2</sub> NPs by hydrolyzing TEOS. 0.5 mL CaCO<sub>3</sub> particle suspension, was mixed with 330 μL of ammonium hydroxide solution, 1660 μL of H<sub>2</sub>O and 8 mL ethanol, after which 46 μL of TEOS was introduced dropwise to the system under magnetic stirring at 700 rpm with the temperature kept at 50 °C for 30 mins. The solution was then stirred at a steady speed of 500 rpm for 20 h at 25 °C. Subsequently, the suspensions were centrifuged and washed with

ethanol and distilled water several times. Finally,  $\text{CaCO}_3/(\text{PAH/PSS})_4$ ,  $\text{CaCO}_3/(\text{PAH/PSS})_6$ ,  $\text{CaCO}_3/(\text{PAH/PSS})_4/\text{SiO}_2$  and  $\text{CaCO}_3/(\text{PAH/PSS})_6/\text{SiO}_2$  were obtained.

**2.3 Harsh acid and alkali treatment.** To test the pH-stability,  $\text{CaCO}_3$  particles with different coating shells was treated with EDTA (0.2 M) and HCl (pH=1).  $(\text{PAH/PSS})_6$  and  $(\text{PAH/PSS})_6/\text{SiO}_2$  capsules were incubated in NaOH (pH=13) for various time (0-24h). After the treatment, the corresponding suspensions were centrifuged, washed and collected for further characterization. It shall be mentioned that all samples were prepared and treated at least 3 times to ensure the repeatability.

**2.4 Ultrasonic treatment.** Ultrasonic treatment was performed by an ultrasonic processor GEX 750 (Sonics & Materials, Inc., USA) operating at 20 kHz, 50 W, and 30% amplitude. The probe of the ultrasonicator was inserted into the particle suspension in a plastic tube. An ice bath was used to ensure that the temperature change of the microcapsule suspensions was less than 5 °C.

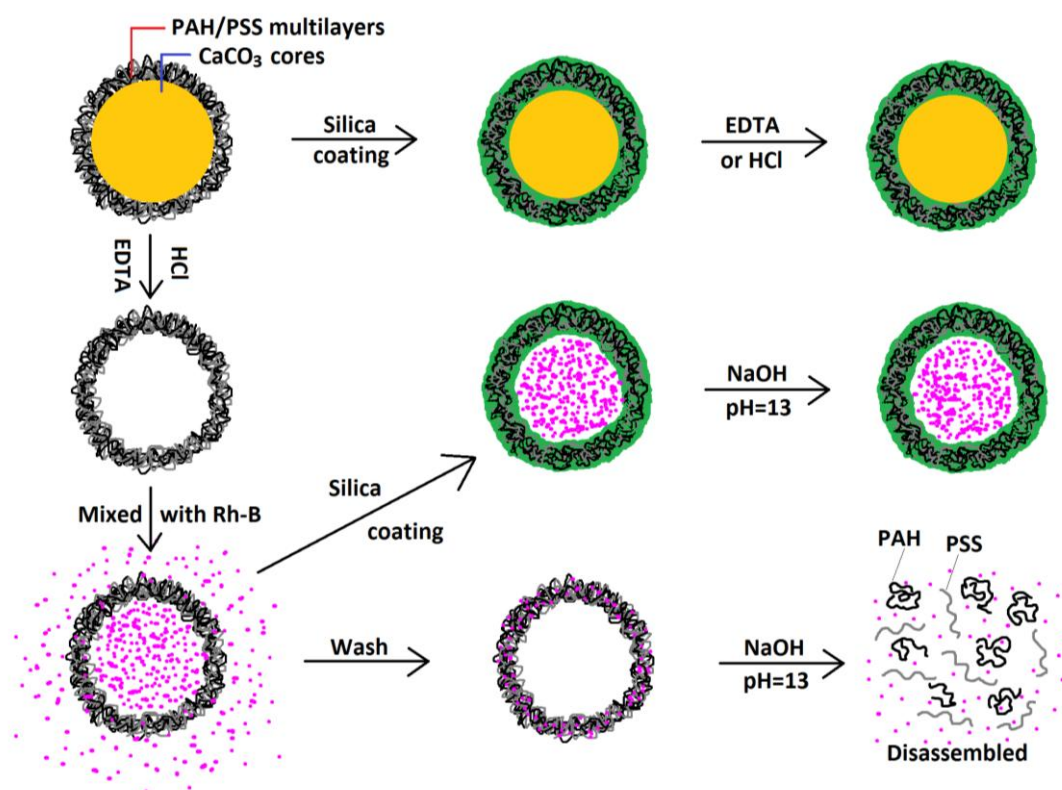
**2.5 Instrument and Measurement.** *Scanning electron microscopy (SEM)* (FEI Inspect-F) was used to measure the morphologies of the samples. The observation was carried out using an accelerating voltage of 10 kV, a spot size of 3.5, and a working distance of approximately 10 mm. Element mapping was characterized by the *Energy dispersive spectrometer (EDX)* attached to the SEM. *Transmission electron microscopy (TEM)* measurements were carried out using a JEOL 2010 transmission electron microscope with a LaB6 filament, operated at 200 kV. Samples were prepared by dropping the diluted sample suspension on a copper grid with holey carbon film and leaving them dry for 5 minutes. *Energy dispersive spectrometer (EDX)* attached to the TEM was employed for the elemental analysis. *Infrared spectroscopy (FTIR spectrometer 100, PerkinElmer)* was used to measure the FTIR spectra of vacuum-dried samples, collecting data at a spectral resolution of 4  $\text{cm}^{-1}$ . *Confocal laser scanning*



*microscopy (CLSM)* images were obtained with a Leica TS confocal scanning system (Leica, Germany) equipped with a 63×/1.4 oil immersion objective.

### 3. Result and Discussion

#### 3.1 Schematic of Protective Shell Synthesis and Harsh Acid/Alkali Treatment



**Scheme 1.** Schematic diagram of the synthesis of PAH/PSS/SiO<sub>2</sub> composite shell and the possible response upon harsh acid/alkali treatment.

Composite polymer/SiO<sub>2</sub> shells were synthesized *via* a synergy of LbL self-assembly and sol-gel method. The scheme of the shell formation and treatment is depicted in Scheme 1. CaCO<sub>3</sub> microparticles were assembled with PAH and PSS alternatively, forming flexible PAH/PSS multilayers, which further served as a scaffold with many nucleating points for the silicification reaction. The formation and growth rates of the incorporated silica are greatly dependant on the system parameters including reaction temperature, concentration of the precursors, reaction time, etc., thus directly affecting the formed composite shell. The

influence of these key parameters was investigated in detail as is highlighted by reference 16. In this study, the best reaction conditions for *in situ* silica incorporation were chosen and implemented.

Two experiments were carried out to investigate the properties of the composite shell. The formed  $\text{CaCO}_3/\text{PAH}/\text{PSS}$  particles were directly coated with silica NPs upon addition of TEOS, forming a complete, uniform, concrete-like outer shell via processes of hydrolyzation and condensation. The capability of the composite  $\text{PAH}/\text{PSS}/\text{SiO}_2$  shells to withstand  $\text{CaCO}_3$  dissolution upon treatment with HCl or the weak acid EDTA (great chelating effect for  $\text{Ca}^{2+}$ ) were then studied. For the reserach on the shell's stability in basic conditions,  $\text{CaCO}_3$  is not an ideal model material as it does not dissolve in NaOH, thus making it difficult to indentify any defects or breakages of the shell encasing the solid  $\text{CaCO}_3$  particles. A fluorescent dye, Rh-B, was used instead. Without silica shielding,  $\text{CaCO}_3$  cores were easily removed by incubating  $\text{CaCO}_3/\text{PAH}/\text{PSS}$  particles in EDTA solution or acid solution, as has been demonstrated elsewhere.<sup>[16]</sup> The  $\text{PAH}/\text{PSS}$  capsules can not seal small molecules within their cavities due to the intrinsic high shell permeability.<sup>[20]</sup> If the  $\text{PAH}/\text{PSS}$  capsules are dispersed in a solvent together with Rh-B, and modified them with *in situ* formed silica NPs, the resultant  $\text{PAH}/\text{PSS}/\text{SiO}_2$  capsules are expected to be able to seal Rh-B within their cavities. It is expected that, the harsh condition tolerance, mechanical strength and long-term storage stability of composite capsules are all notably improved due to the shielding effect of the inorganic NPs, compared to pure polymeric multilayers.<sup>[16,25]</sup> The effects of high pH on  $\text{PAH}/\text{PSS}/\text{SiO}_2$  capsules can be analyzed by detecting whether Rh-B molecules were able to escape to the outside. Hence, the stability and permeability of pure  $\text{PAH}/\text{PSS}$  capsules and the composite  $\text{PAH}/\text{PSS}/\text{SiO}_2$  capsules under alkaline conditions were investigated in the manner illustrated in Scheme 1. It is believed that the composite shell would keep an intact

morphology and maintain the capacity to encapsulate Rh-B. The detailed results and investigation are discussed as follows.

### 3.2 Performance Under Acid Treatment

In order to clearly characterize  $\text{CaCO}_3$  particles by fluorescent images, TRITC-dextran molecules (500 kDa) were loaded into the  $\text{CaCO}_3$  cores *via* co-precipitation process and the formed particles were characterized by SEM and CLSM, as shown in Figure S1. SEM image in Figure S1 A (Supporting Information) indicates that the freshly synthesized  $\text{CaCO}_3$  particles are micro-sized and show quite rough surfaces. Due to the diffusion-limited permeation inside the  $\text{CaCO}_3$  particles and the adsorption of TRITC-dextran molecules on pore surfaces, TRITC-dextran is expected to be effectively loaded in the  $\text{CaCO}_3$  particles.<sup>[33]</sup> CLSM images in Figure S1 B and C (Supporting Information) confirm that TRITC-dextran molecules are embedded inside the  $\text{CaCO}_3$  particles and display a uniform distribution.

As it is well-known that  $\text{CaCO}_3$  can be dissolved by acid, a protective shell is needed to preserve their stability in acidic solvents for some real cases. Here, three types of shells with different compositions were used to coat the  $\text{CaCO}_3$  loaded with TRITC-dextran: (i) pure polymeric shells,  $(\text{PAH/PSS})_6$ ; (ii) pure inorganic shells,  $\text{SiO}_2$ ; and (iii) polymeric-inorganic composite shells,  $(\text{PAH/PSS})_6/\text{SiO}_2$ .  $\text{CaCO}_3$  particles with 6 PAH/PSS bilayers and composite  $(\text{PAH/PSS})_6/\text{SiO}_2$  shell before and after acid treatment were characterized by SEM and CLSM. Figure 1 A shows that the surface roughness of  $\text{CaCO}_3/(\text{PAH/PSS})_6$  reduces significantly compared with that of bare  $\text{CaCO}_3$  particles (Figure S1 A, Supporting Information), indicating that the polymeric building blocks are successfully assembled on their surfaces. The filled red spheres in CLSM images in Figure 1 A2 reveal that the encapsulated TRITC-dextran molecules are sealed well during the coating process and still distribute uniformly in the cores.

After incubating these  $\text{CaCO}_3/(\text{PAH/PSS})_6$  in weak acid solution, i.e., 0.2 M EDTA, the  $\text{CaCO}_3$  cores are completely removed, as verified by the SEM image in Figure 1 B1, showing film-like  $(\text{PAH/PSS})_6$  microcapsules with a lot of wrinkles and folds. Without the support of  $\text{CaCO}_3$  cores,  $(\text{PAH/PSS})_6$  multilayers are soft and collapsed during the drying process due to the interior water evaporation (Figure 1 B1), which supports the theory provided in the previous reports.<sup>[16,20]</sup> CLSM image in Figure 1 B2 shows hollow bright red rings, indicating that the  $\text{CaCO}_3$  are dissolved and that most of the TRITC-dextran molecules are enriched around the interior PAH/PSS shells. The inset in Figure 1 B2 confirms this point, as the capsules exhibit near zero unit inside the cavities and relative high intensity in the shells. The absorption of TRITC-dextran in shells can be explained by the possible interaction between PAH and dextran, which can be facilitated by both hydrogen bonds and hydrolyzable covalent cross-links resulted from aldehydes and primary amines coupling.<sup>[35]</sup> The results indicate that pure PAH/PSS (6 bilayers) cannot inhibit the weak acid with small molecular weight, i.e., EDTA, which can penetrate into the porous  $\text{CaCO}_3$ , chelate  $\text{Ca}^{2+}$  ions and thereby dissolve them completely. SEM images of  $\text{CaCO}_3$  particles coated directly with  $\text{SiO}_2$  NPs before and after EDTA treatment are given in Figure S2 (Supporting Information).  $\text{SiO}_2$  NPs covered on the  $\text{CaCO}_3$  surfaces can be clearly seen from Figure S2 A (Supporting Information). Notably, pure  $\text{SiO}_2$  coatings are not dense enough to protect the  $\text{CaCO}_3$  cores, which is proved by the shrink morphology with folds after EDTA treatment (Figure S2 B, Supporting Information). Based on the above discussion, it is apparent that neither the pure polymeric multilayers nor the pure silica coatings are able to protect the  $\text{CaCO}_3$  from being dissolved in acidic condition.

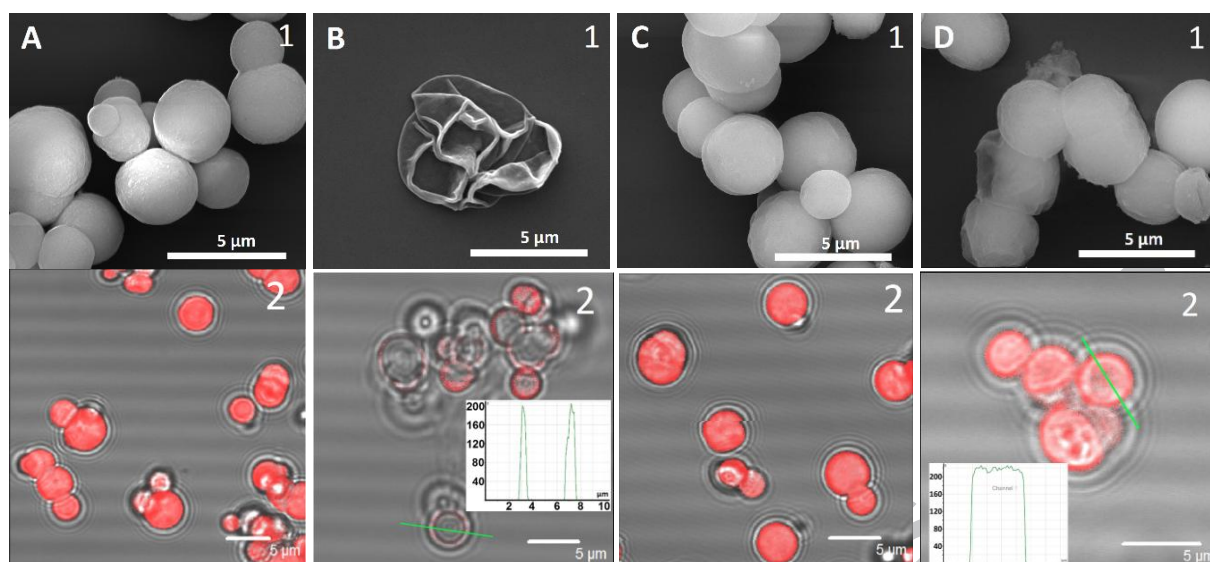


**Figure 1.** SEM (top row) and CLSM (bottom row) images of  $\text{CaCO}_3/(\text{PAH/PSS})_6$  without and with silica coating, before and after EDTA treatment: (A)  $\text{CaCO}_3/(\text{PAH/PSS})_6$ ; (B)  $\text{CaCO}_3/(\text{PAH/PSS})_6$ , EDTA; (C)  $\text{CaCO}_3/(\text{PAH/PSS})_6/\text{SiO}_2$ ; (D)  $\text{CaCO}_3/(\text{PAH/PSS})_6/\text{SiO}_2$ , EDTA. The line scan inset shows relative fluorescent intensity in capsules.

Previous reports have demonstrated that one polyelectrolyte bilayer is soft, porous, and only less than 3 nm in thickness,<sup>[34]</sup> however, the decoration of *in situ* synthesized inorganic  $\text{SiO}_2$  NPs in the polymeric matrix can empower the formed composite shell with enhanced mechanics, increased shell thickness and reduced permeability.<sup>[16]</sup> Hence, the polymeric/inorganic composite shell is expected to be able to protect  $\text{CaCO}_3$  upon acid treatment. Figure 1 C1 reveals that the particles with a spherical shape are fully covered by the composite  $(\text{PAH/PSS})_6/\text{SiO}_2$  shells. CLSM images in Figure 2 C2 prove a uniform distribution of the captured TRITC-dextran. Around 80% of the particles are found in SEM image (Figure 2 D1) and they still keep 3D free-standing morphology without collapse after the EDTA treatment. However this is insufficient to prove that these spherical particles maintain solid  $\text{CaCO}_3$  cores inside, because previous reports have demonstrated that hollow composite capsules may also display a free-standing structure under dry state due to the increased mechanics and shell thickness.<sup>[16]</sup> Therefore, CLSM and TEM images were

measured to study whether  $\text{CaCO}_3$  particles are intact. The corresponding CLSM results show that most of the particles are solid red balls and the line scan inset reveals the fluorescence intensity of  $\sim 220$  units inside the capsule, which confirms the existence of  $\text{CaCO}_3$  cores with pre-loaded TRITC-dextran (Figure 1 D2). In addition, to further prove that most of  $\text{CaCO}_3$  are protected from dissolving, TEM of  $\text{CaCO}_3/(\text{PAH/PSS})_6/\text{SiO}_2$  after incubating in EDTA solution was measured, as shown in Figure 2 A and B. Only one hollow particle is found, and other particles are solid and fully coated by  $\text{PAH/PSS/SiO}_2$  shells. The thickness of the composite shell is around 295 nm as illustrated in Figure 2 B, which is more than 10 times thicker than that of pure  $(\text{PAH/PSS})_6$  multilayers.<sup>[34]</sup> EDX spectra obtained from different particles are give alongside the TEM images in Figure 2 C and D. No Ca peak is found for the hollow particle in Figure 2 C. However, for solid particle, there is a very strong Ca peak originating from  $\text{CaCO}_3$  in Figure 2 D where other peaks are attributed to C, O, S, Cu and Si. Among them, the peak of S originates from the original PSS and the peaks of Cu comes from the copper TEM grid. Moreover, the peaks of Si further verify the formation of  $\text{SiO}_2$  NPs. The element mapping of  $\text{CaCO}_3$  coated with  $(\text{PAH/PSS})_6/\text{SiO}_2$  after soaking in EDTA is shown in Figure S3 (Supporting Information), which further confirms that most of the particles are solid particles with  $\text{CaCO}_3$  core inside.



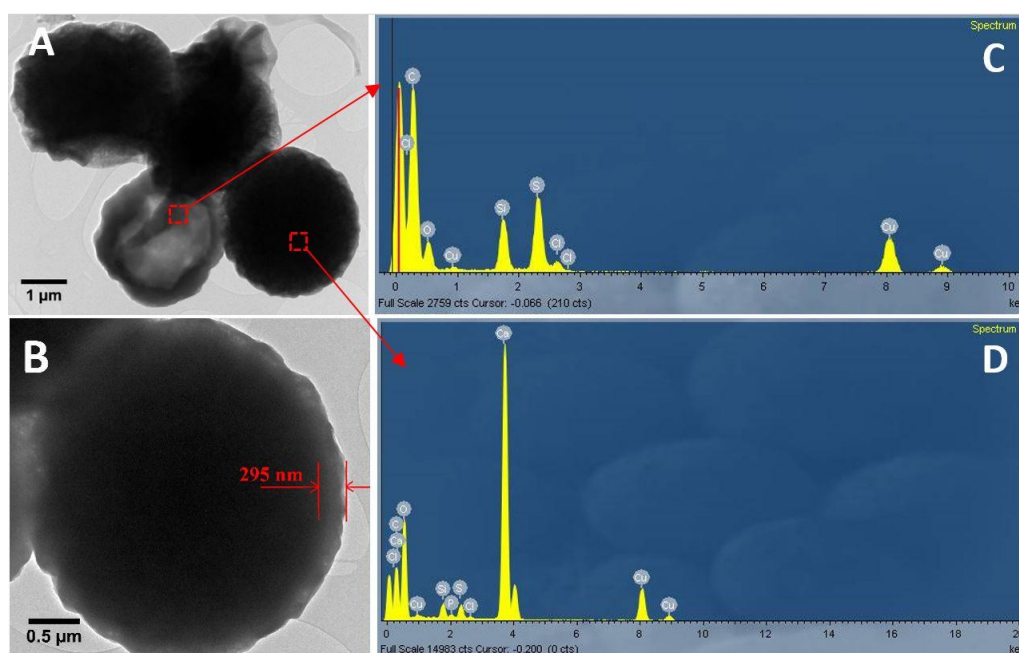


**Figure 2.** TEM images (A, B) and EDX spectra (C, D) of  $\text{CaCO}_3/(\text{PAH/PSS})_6/\text{SiO}_2$  after EDTA treatment. Image C corresponds to the EDX spectrum obtained from the hollow particle and image D corresponds to the solid particle.

It shall be mentioned that the layer number of the polyelectrolytes remarkably affects their stability under harsh conditions. The results of  $\text{CaCO}_3$  with 4 PAH/PSS layers are shown in Figure S4-S6 (Supporting Information). Figure S5 A indicates that the composite shell with 8 polymer layers is only around 130 nm, which is much smaller than that of the  $\text{CaCO}_3/(\text{PAH/PSS})_6/\text{SiO}_2$  shell. Even though the  $(\text{PAH/PSS})_4/\text{SiO}_2$  composite shell shows an increased protective effects for  $\text{CaCO}_3$  when compared with pure  $(\text{PAH/PSS})_4$  multilayers, nearly half of the cores are removed by EDTA, as indicated by the CLSM images in Figure S4 D, Figure S5 and Figure S6 (Supporting Information).

The FTIR spectra of  $\text{CaCO}_3$  and the  $\text{CaCO}_3/(\text{PAH/PSS})_6/\text{SiO}_2$  after EDTA treatment were recorded, Figure 3. For pure  $\text{CaCO}_3$ , three main absorption bands appears at  $\sim 1400$ ,  $\sim 870$  and  $\sim 712 \text{ cm}^{-1}$ , which are characteristic bands of calcite. These bands obviously exist in the

sample of  $\text{CaCO}_3/(\text{PAH/PSS})_6/\text{SiO}_2$ , and display a relatively higher intensity than those of  $\text{CaCO}_3/(\text{PAH/PSS})_4/\text{SiO}_2$  after EDTA treatment (Figure S6, Supporting Information). The bands at around  $1100\text{ cm}^{-1}$ ,  $945\text{ cm}^{-1}$  as well as  $800\text{ cm}^{-1}$  for the composite particles are attributed to the Si–O–Si and Si–OH bonds, which also confirm the formation of  $\text{SiO}_2$  NPs.

[15,25]

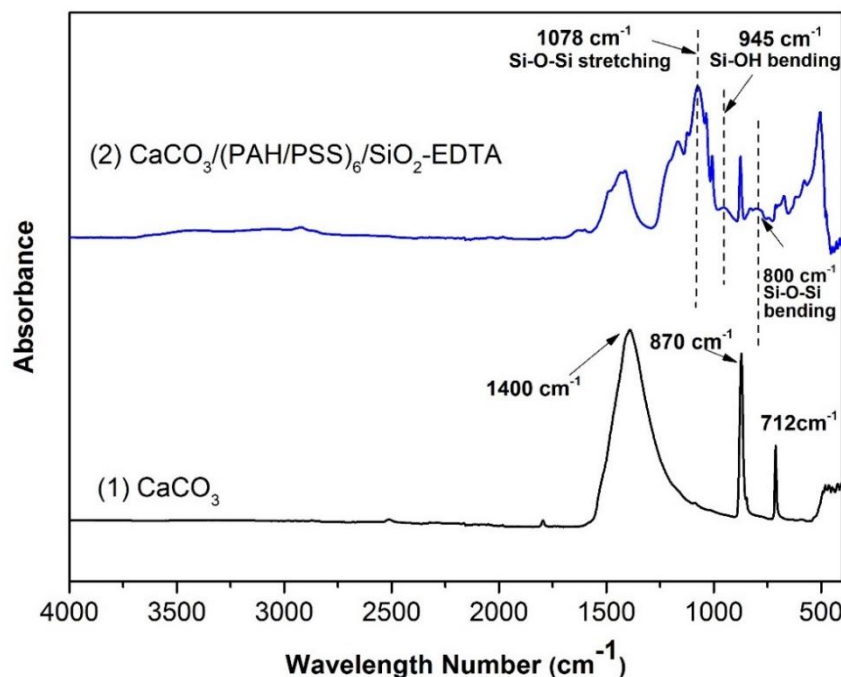


**Figure 3.** FTIR spectrums pure  $\text{CaCO}_3$  and  $\text{CaCO}_3/(\text{PAH/PSS})_6/\text{SiO}_2$  after EDTA treatment.

As demonstrated above, with 12 layers of polymer and one cycle of  $\text{SiO}_2$  coating, the  $\text{CaCO}_3$  particles can be protected from being dissolved by EDTA. Additional investigation were carried out to study their tolerance to extreme acidic condition (HCl solution with  $\text{pH}=1$ ).

The  $\text{CaCO}_3/(\text{PAH/PSS})_6/\text{SiO}_2$  particles were incubated in 1 M HCl ( $\text{pH}=1$ ) for 2 minutes and characterized by SEM and TEM. Figure 4 A shows that most of the particles are spheres with a slightly rough surface after HCl treatment. If the particles were cut randomly by knife, some broken particles can be found, as shown in Figure 4 B and C. The porous structures of the undissolved  $\text{CaCO}_3$  cores are demonstrated in Figure 4 B. Broken hollow particles in Figure 4



C reveal the thick composite shell, around 300 nm, which is similar with that calculated from the TEM images in Figure 2 B and Figure 4 F. Solid particle found in the TEM images confirms that most of the  $\text{CaCO}_3$  cores protected by  $(\text{PAH/PSS})_6/\text{SiO}_2$  shells are not removed by HCl. Therefore, we can conclude that  $\text{CaCO}_3$  with  $(\text{PAH/PSS})_6/\text{SiO}_2$  coating possesses a good stability under acidic environment, since most of the  $\text{CaCO}_3$  particles are protected by the thick and dense composite shells. In addition, it is worth pointing out the existence of some hollow particles in the system, as indicated in the SEM, TEM and CLSM images in Figure 1, Figure 2 and Figure 4. This can be explained by the occurrence of defects in the composite shells for small proportion particles, resulted from some possible alteration or fluctuation of the reaction parameters such as the environment temperature during the silica coating process. The hybrid shells with defects can not intercept small molecules and prevent them from going through the shell, thereby cannot effectively protect the  $\text{CaCO}_3$  cores.

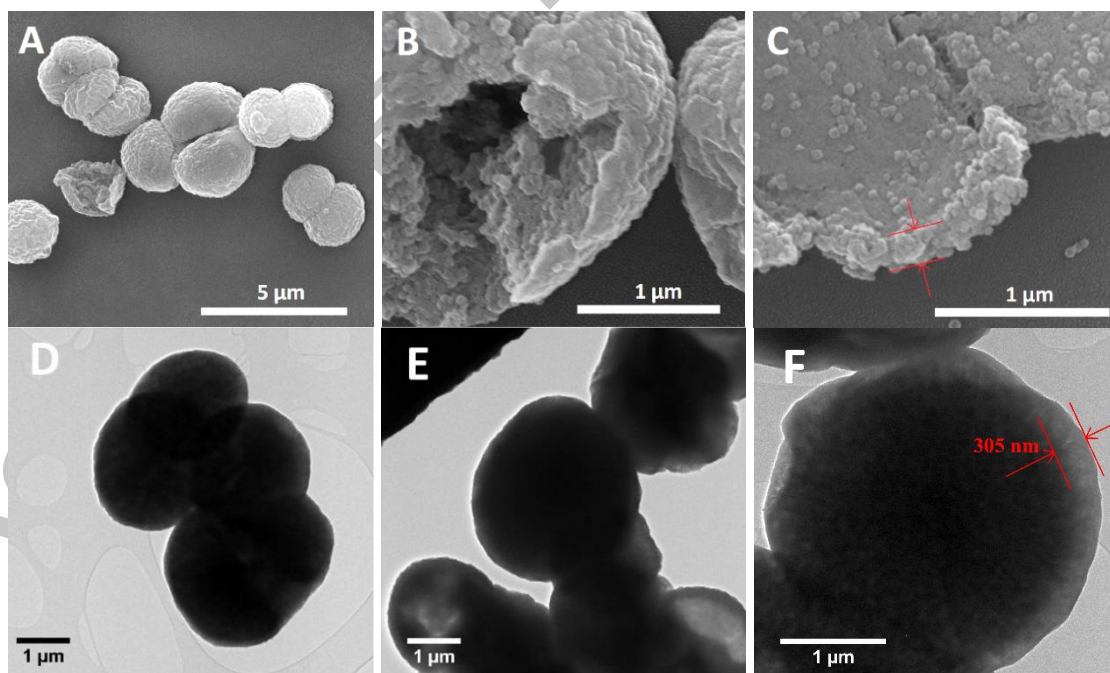


**Figure 4.** SEM (A, B, C) and TEM (D, E, F) images of  $\text{CaCO}_3/(\text{PAH/PSS})_6/\text{SiO}_2$  after 2 mins of incubation in 1 M HCl treatment.

### 3.3 Performance Under Alkaline Treatment

The (PAH/PSS)<sub>6</sub> multilayers without and with SiO<sub>2</sub> incorporation were subjected to harsh alkali conditions to test their stability and responsive behaviour. As mentioned above, the possible damage of (PAH/PSS)<sub>6</sub> and (PAH/PSS)<sub>6</sub>/SiO<sub>2</sub> induced by NaOH are hardly recognized and characterized by SEM and CLSM measurement if they were coated on solid CaCO<sub>3</sub> particles, because NaOH can not dissolve CaCO<sub>3</sub> cores. Therefore, hollow (PAH/PSS)<sub>6</sub> microcapsules without and with SiO<sub>2</sub> decoration were employed to study the tolerance to extreme basic conditions. Figure 5 shows the SEM images of original (PAH/PSS)<sub>6</sub> capsules and the ones after soaking in NaOH solution (pH=13). The results indicates that with only 2 seconds of treatment, all the capsules are completely disassembled into flocculated sludge (Figure 5 B). Such results proved that pure PAH/PSS multilayers are not stable in solvents with a high pH value.

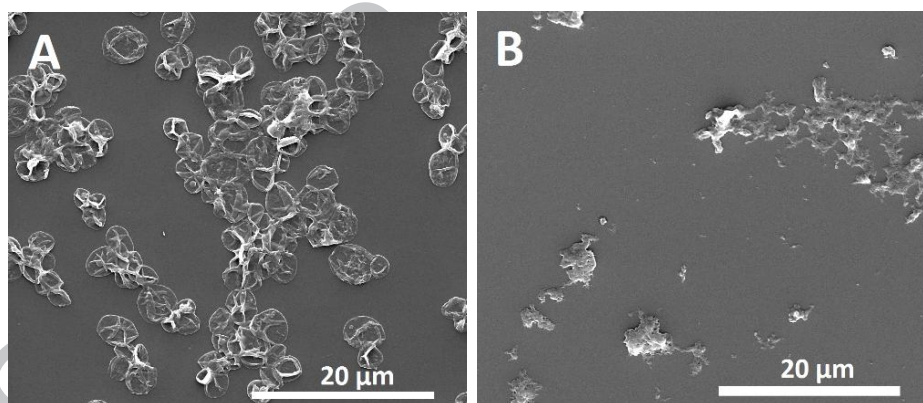


**Figure 5.** SEM images of pure (PAH/PSS)<sub>6</sub> capsules before (A) and after (B) being soaked in NaOH (pH=13) for 2 seconds.

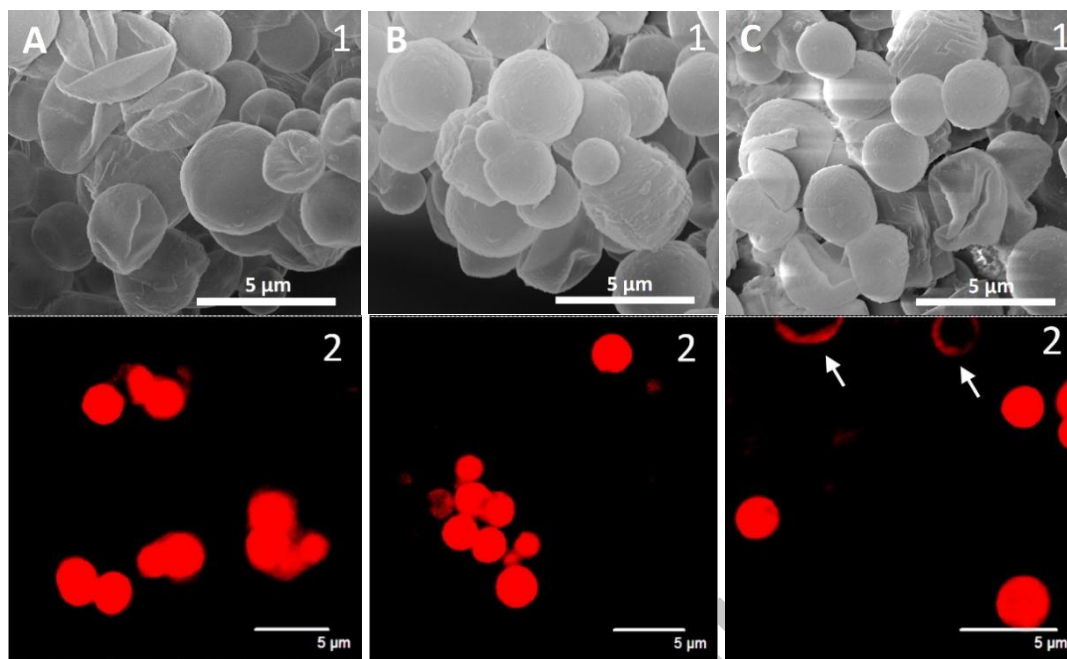


**Figure 6.** SEM (top row) and CLSM (bottom row) images of  $(\text{PAH/PSS})_6/\text{SiO}_2$  capsules loaded with Rh-B and treated with NaOH solution (pH=13) for (A) 0 min, (B) 10 mins and (C) 1 h.

Subsequently, the performance of composite shell in NaOH solution (pH=13) was investigated by employing  $(\text{PAH/PSS})_6/\text{SiO}_2$  capsules loaded with small molecules, Rh-B. As shown in Scheme 1, Rh-B were sealed inside their cavities during the silica coating process. Different from the flattened  $(\text{PAH/PSS})_6$  microcapsules without  $\text{SiO}_2$  coating, Figure 6 A1 shows that  $(\text{PAH/PSS})_6/\text{SiO}_2$  capsules are strong enough to be intact and remain their spherical morphology under the dry state. Their CLSM image in Figure 6 A2 confirms the efficient encapsulation of Rh-B molecules. Rh-B should diffuse outside easily if any defects or cracks appear which might induced by NaOH soaking. After 10 mins of soaking with NaOH, no change in morphology is found in the SEM image, Figure 6 B1. It seems that all the Rh-B molecules are still sealed firmly inside the capsules as most of the capsules in the CLSM image are filled red balls, as illustrated in Figure 6 B2. When prolonging the time to 1 h, no significant changes in morphology appear, as verified by the SEM image in Figure 6

C1. For the encapsulation behaviour, the CLSM image in Figure 6 C2 indicates that some of the capsules lose the encapsulation property, showing as hollow red ring indicated by arrows. But there are still more than 50% of the capsules maintained Rh-B molecules. When further prolonging the soaking time to 4 h, some morphology changes can be identified from the SEM image in Figure S7 B (Supporting Information), showing big aggregated particles on the shell surface. The composite capsules collapse and are destroyed to a large extent after 24 h of incubation in NaOH, Figure S7 C (Supporting Information). Compared with poor stability in extreme basic solution for PAH/PSS multilayers, it is obvious that the incorporation of *in situ* formed SiO<sub>2</sub> NPs into the (PAH/PSS)<sub>6</sub> matrix significantly improves its stability in basic condition, demonstrated by the 4 hours maintenance of morphology and structure in NaOH solution (pH=13).

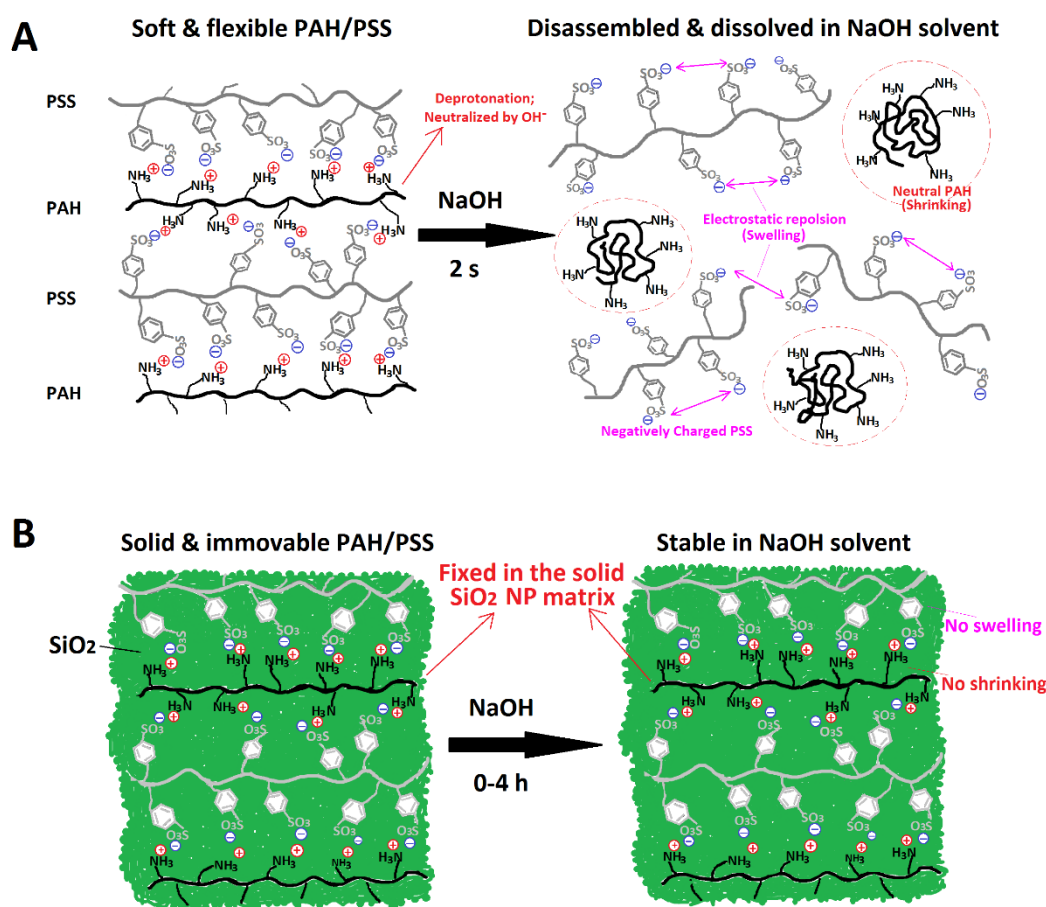
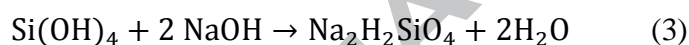
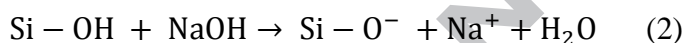


**Figure 7.** Mechanism models of (A) disassembly of PAH/PSS upon NaOH treatment and (B) intact behaviour of PAH/PSS/SiO<sub>2</sub> upon NaOH treatment. The incorporated silica NPs concrete together as a solid and dense matrix, fixing the soft PAH and PSS inside it.

Figure 7 depicts the possible mechanism models for the capsules without and with SiO<sub>2</sub> NPs coating under NaOH treatment. For the pure PAH/PSS capsules, the pH of the solution affects the interaction (attractive or repulsive) between the two oppositely charged PAH and PSS and consequently changed the multilayer structure.<sup>[17,36]</sup> Specially, as shown in Figure 7 A, at pH 7 (DI-water as solvent) both polyelectrolytes are highly charged, and there is a global compensation of charges between the polycation and the polyanion. The PAH and PSS molecules are assembled together and form stable but soft multilayer capsules. When the PAH/PSS multilayers were incubated in NaOH solvent with pH=13, which is higher than the pK<sub>a</sub> of polybases, i.e. PAH (pK<sub>a</sub>=10.8), the assembled PAH becomes uncharged and coiled thus resulting in the disassembly of the capsules.<sup>[18,36]</sup> In addition, due to the high concentration of OH<sup>-</sup> ions, the intramolecular and intermolecular electrostatic repulsion of the assembled PSS molecules increases, leading to their swelling and dissociation of PSS molecules in the solvent from the multilayers, which also promotes the disassembly process.<sup>[37]</sup> In terms of the composite PAH/PSS/SiO<sub>2</sub> shells, the SiO<sub>2</sub> inorganic NPs are *in situ* formed and introduced into the polymer multilayers by a one-step sol-gel approach. Different from the addition of pre-prepared inorganic NPs in polymeric multilayers, the incorporated silica NPs integrate with each other as well as the soft polymer, forming a continuous, homogenous, dense and intact hybrid shell.<sup>[16]</sup> As shown in Figure 7 B, the soft PAH and PSS molecules are coagulated and fixed by the solid SiO<sub>2</sub> building blocks, and thus could not rotate or move. Therefore, the changes of the electrostatic attractive forces between the polymeric layers, i.e., PAH and PSS, and that of the force between the polymeric building blocks and inorganic SiO<sub>2</sub> particles is likely to be negligible when the external environmental

ionic conditions change. It is demonstrated by the intact morphology and structure of the composite capsules upon modifying the pH value in the range from 1 to 13 with a certain period of treatment time. Notably, when treating the (PAH/PSS)<sub>6</sub>/SiO<sub>2</sub> with concentrated NaOH (pH=13) for 1 h, some capsules lose the small molecule encapsulation property (Figure 6 C2) even though they still keep their morphology unchanged. Because the hydroxyl ions (OH<sup>-</sup>) in the solvent are given plenty of time to attack the incorporated non-crystalline silica, reacting with Si-O-Si and the hydroated silica (e.g., Si-OH). Possible reactions are shown as following: <sup>[38,39-41]</sup>



Usually, when the composite shell contacts with water, hydrolysis reaction (1) happens and results that the surface of silica particles is covered with a thin layer of Si-OH. <sup>[38,39-41]</sup> Reaction (1) occurs in water, but it is catalysed by hydroxyl ions and is completed only in sufficiently alkaline solutions. <sup>[40]</sup> Hence, with base catalysis, more and more silica hydrolyzes into Si-OH, Si(OH)<sub>2</sub>, Si(OH)<sub>3</sub> and Si(OH)<sub>4</sub>. Such hydroated silica will quickly react with hydroxyl ions, as exemplified in reaction (2) and (3), which may promote the connection and merge between individual silica NPs and result a swelling to some degree. <sup>[39,41]</sup> The deprotonation of hydroated silica and the consequent formation of dissolvable Si-O<sup>-</sup> and Na<sub>2</sub>H<sub>2</sub>SiO<sub>4</sub> facilitates the detachment of silica into the solution. In this study our results demonstrate that the composite capsules do not show any obvious change in their morphology and permeability, when incubated in NaOH solution at 25 °C for less than 4 h. This is due to that the hybrid structure of polymers and silica is condensely packed and integrated. The polymeric buliding blocks inhibit the hydrolysis and dissolve process of silica particles upon the attack of hydroxyl ions. Simultaneously, the densely packed silica NPs provent the rotation and disassembly of PAH/PSS upon high OH<sup>-</sup> ions attack. It shall be noted,



however, that some defects may appear in the composite shell during the reaction processes, which results in the release of Rh-B molecules as demonstrated by the red rings in the CLSM image in Figure 6 C2. With prolonging the treatment time, more silica NPs react with NaOH. When the time approaching 24 h, the amount of the soluble sodium silicates such as  $\text{Na}_2\text{H}_2\text{SiO}_4$  is increased significantly, leading to the appearance of obvious defects and even complete disruption of the composite shells. Hence, nearly no intact capsules are found in Figure S7 C (Supporting Information).

### 3.4 Ultrasound Responsive Properties

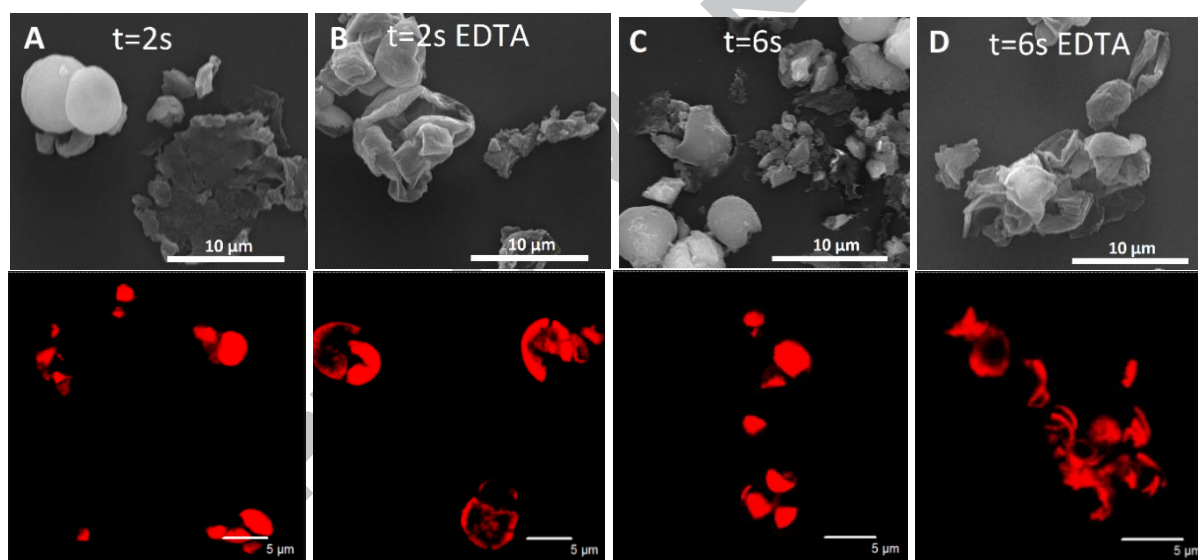


**Figure 8.** SEM images (top row) and confocal fluorescent images (bottom row) of  $\text{CaCO}_3/(\text{PAH/PSS})_6/\text{SiO}_2$  with 2 s (A, B) and 6 s (C, D) of ultrasonication before (A, C) and after (B, D) EDTA treatment.

For the controlled release of cargo from the composite shells, ultrasound, which is already employed as a diagnostic and therapeutic method for many diseases, is a promising trigger due to its long penetration depth and low invasive nature. As demonstrated previously, composite shells with inorganic NPs possess a higher sensitivity to ultrasonication when

compared with soft polymer shells. This is due to the fact that inorganic NPs empower the formed shells with an increased stiffness, therefore increasing the density gradient across the water/shell interface, consequently improving the absorption of acoustic energy.<sup>[16,29]</sup> Here, we treated the  $\text{CaCO}_3/(\text{PAH/PSS})_6/\text{SiO}_2$  particles with ultrasound (GEX 750, Sonics & Materials, Inc., USA, 20 kHz, 50 W, 30% amplitude). SEM images of the particles after different sonication times are displayed in Figure 8, demonstrating that the ultrasound waves can break the composite  $(\text{PAH/PSS})_6/\text{SiO}_2$  shells and even rupture the solid  $\text{CaCO}_3$  cores. With 2 s of ultrasonication, some particles still show an intact morphology, as indicated by the arrows in Figure 8 A. The solid fluorescent balls in CLSM images further prove the existence of  $\text{CaCO}_3$  cores. However, such results can not prove that the composite shells covering the intact  $\text{CaCO}_3$  cores are not destroyed by the ultrasound treatment. Incubating them in EDTA solution was then carried out. All particles collapse and it seems that no cores maintain intact after EDTA treatment, Figure 8 B. The corresponding CLSM image indicates that there are only broken shells and no filled fluorescent spheres are found. If prolonging the ultrasonication time to 6 s, the size of fragments decreases and almost no particles are found with an intact spherical shape, as proved by the SEM image in Figure 8 C. After EDTA treatment, the broken composite  $(\text{PAH/PSS})_6/\text{SiO}_2$  shells are left without any  $\text{CaCO}_3$  particles, which can be clearly seen from the CLSM image in Figure 8 D. However, with only 6 PAH/PSS bilayers of coating, the  $\text{CaCO}_3$  particles are not broken by 6 s of ultrasonication, as shown in Figure S8 A (Supporting Information), which indicates that the polymeric shells possess a lower sensitivity to ultrasound compared with the composite shells. After soaking with EDTA, all  $\text{CaCO}_3$  cores are removed, leading to  $(\text{PAH/PSS})_6$  microcapsules with some defects as indicated by the arrows in Figure S8 B (Supporting Information). In general, here we demonstrate that the composite shells have the ability to resist chemical attack, especially to the extreme acidic (pH=1) and basic (pH=13) conditions, which is important for the design of drug carriers, biosensing systems, and composite NPs for oil/gas recovery



applications.<sup>[12,42,43]</sup> Ultrasound waves can be used as a tool to open the composite shell and enable release of the entrapped particles or molecules. Thereby, the polymeric-inorganic composite (PAH/PSS)<sub>6</sub>/SiO<sub>2</sub> shells present a promising platform for stable and tunable microcontainers for encapsulation of small molecules, large macromolecules, nanoparticles, cells, and other species, for protection during their delivery process, and for their controlled release in areas of interest upon external ultrasound treatment.

#### 4. Conclusion

Our study demonstrates a combined LbL assembly and sol-gel method for synthesizing polymeric/inorganic composite shells with excellent tolerance to harsh acidic and alkali conditions ( $1 \leq \text{pH} \leq 13$ ). The (PAH/PSS)<sub>6</sub>/SiO<sub>2</sub> composite shells are denser, thicker and more stable than (PAH/PSS)<sub>6</sub> shells, showing the ability to prevent the encapsulated CaCO<sub>3</sub> particles from being dissolved by EDTA and HCl, and the feasibility to seal small molecules (e.g., Rh-B) inside to protect them under extreme basic condition with pH=13 for a relatively long time. The thickness of the (PAH/PSS)<sub>6</sub>/SiO<sub>2</sub> shell reaches to ~ 300 nm. The SEM, TEM and CLSM data reveal that most of the CaCO<sub>3</sub>/(PAH/PSS)<sub>6</sub>/SiO<sub>2</sub> particles are maintained an intact morphology and solid structure after acid treatment. Under the harsh basic environment, (PAH/PSS)<sub>6</sub> multilayers are found to quickly disassemble after only 2 s of incubation in NaOH (pH = 13) due to deprotonation of amino groups at PAH. In contrast, the composite shells, (PAH/PSS)<sub>6</sub>/SiO<sub>2</sub>, display an intact morphology for 4 h upon NaOH treatment, which demonstrates their enhanced stability and excellent tolerance to harsh basic conditions. In addition, CLSM images prove the ability of composite shells to encapsulate Rh-B and to protect them for 4 hours long. To break the composite shells and release the encapsulated substance, ultrasound can be used as one potential tool. Such composite (PAH/PSS)<sub>6</sub>/SiO<sub>2</sub> shells with a higher chemical stability and a lower permeability could be potentially used for various applications where protecting the activity of small molecules in extreme conditions

and allowing their controlled and triggered release is required. Further works will focus on encapsulation and delivery of pH-sensitive drugs by such composite shells, or developing controlled surfactant delivery systems which are tolerance to subsurface conditions.

### Acknowledgement

H.G. appreciates financial support from China Scholarship Council for her Ph.D. study.

### Supplementary Materials

SEM and CLSM images of  $\text{CaCO}_3$  particles loading with TRITC-dextran; SEM images of  $\text{CaCO}_3$  particles coated with pure silica NPs; EDX mapping profiles of  $\text{CaCO}_3/(\text{PAH/PSS})_6/\text{SiO}_2$  after EDTA treatment; SEM, CLSM and TEM images of  $\text{CaCO}_3/(\text{PAH/PSS})_4$  and  $\text{CaCO}_3/(\text{PAH/PSS})_4/\text{SiO}_2$  before and after EDTA treatment; FTIR profiles of  $\text{CaCO}_3/(\text{PAH/PSS})_4/\text{SiO}_2$  after EDTA treatment; Morphology characterization of  $(\text{PAH/PSS})_4/\text{SiO}_2$  capsules after incubating in NaOH (pH=13) for different time: 5 mins, 4 h and 24 h; SEM and CLSM images of  $\text{CaCO}_3/(\text{PAH/PSS})_4$  treated by 6 s of ultrasound before and after EDTA treatment.

### Corresponding Author

\* E-mail: [h.gao@qmul.ac.uk](mailto:h.gao@qmul.ac.uk) (H.G)

\* E-mail: [g.sukhorukov@qmul.ac.uk](mailto:g.sukhorukov@qmul.ac.uk) (G.B.S.)

### Notes

The authors declare no competing financial interest.

### References

- [1] B. Albertini, M. Di Sabatino, G. Calogera, N. Passerini, L. Rodriguez, J. *Microencapsul.* **2010**, 27, 150.

- [2] E. Oh, K. Susumu, A. J. Makinen, J. R. Deschamps, A. L. Huston, I. L. Medintz, *J. Phys. Chem. C* **2013**, *117*, 18947.
- [3] H. A. Son, S. K. Choi, E. S. Jeong, B. Kim, H. T. Kim, W. M. Sung, J. W. Kim, *Langmuir* **2016**, *32*, 8909.
- [4] M. Jaganathan, D. Madhumitha, A. Dhathathreyan, *Adv. Colloid Interface Sci.* **2014**, *209*, 1.
- [5] R. I. Corona-Hernandez, E. Álvarez-Parrilla, J. Lizardi-Mendoza, A. R. Islas-Rubio, L. A. de la Rosa, A. Wall-Medrano, *Compr. rev. food sci. food saf.* **2013**, *12*, 614.
- [6] M. A. Islam, *J. Microbiol. Biotechnol.* **2010**, *20*, 1367.
- [7] L. Y. Chu, T. Yamaguchi, S. Nakao, *Adv. Mater.* **2002**, *14*, 386.
- [8] G. Lajoinie, E. Gelderblom, C. Chlon, M. Bohmer, W. Steenbergen, N. de Jong, S. Manohar, M. Versluis, *Nat. Commun.* **2014**, *5*, 3671.
- [9] Y. Ma, W. F. Dong, M. A. Hempenius, H. Mohwald, G. J. Vancso, *Nat. Mater.* **2006**, *5*, 724.
- [10] D. Zhao, C. Q. Wang, R. X. Zhuo, S. X. Cheng, *Colloids Surf. B Biointerfaces* **2014**, *118*, 111.
- [11] A. S. Timin, A. R. Muslimov, A. V. Petrova, K. V. Lepik, M. V. Okilova, A. V. Vasin, B. V. Afanasyev, G. B. Sukhorukov, *Sci. Rep.* **2017**, *7*.
- [12] M. Stumpp, M. Y. Hu, Y. C. Tseng, Y. J. Guh, Y. C. Chen, J. K. Yu, Y. H. Su, P. P. Hwang, *Sci. Rep.* **2015**, *5*, 10421.
- [13] S. Fujiki, Y. Iwao, M. Kobayashi, A. Miyagishima, S. Itai, *Chem. Pharm. Bull. (Tokyo)* **2011**, *59*, 553.
- [14] S. Mytnyk, I. Ziemecka, A. G. L. Olive, J. W. M. van der Meer, K. A. Totlani, S. Oldenhof, M. T. Kreutzer, V. van Steijn, J. H. van Esch, *RSC Adv.* **2017**, *7*, 11331.
- [15] Z. S. Al-Garawi, G. E. Kostakis, L. C. Serpell, *J. Nanobiotechnology* **2016**, *14*, 79.
- [16] H. Gao, D. Wen, G. B. Sukhorukov, *J. Mater. Chem. B* **2015**, *3*, 1888.

- [17] K. Yoshida, T. Ono, Y. Kashiwagi, S. Takahashi, K. Sato, J. Anzai, *Polymers* **2015**, 7, 1269.
- [18] M. A. Pechenkin, H. Mohwald, D. V. Volodkin, *Soft Matter* **2012**, 8, 8659.
- [19] V. Kozlovskaya, E. Kharlampieva, M. L. Mansfield, S. A. Sukhishvili, *Chem. Mater.* **2006**, 18, 328.
- [20] H. Gao, A. V. Sapelkin, M. M. Titirici, G. B. Sukhorukov, *ACS Nano* **2016**, 10, 9608..
- [21] A. A. Antipov, G. B. Sukhorukov, E. Donath, H. Mohwald, *J. Phys. Chem. B* **2001**, 105, 2281.
- [22] I. Pastoriza-Santos, B. Scholer, F. Caruso, *Adv. Funct. Mater.* **2001**, 11, 122.
- [23] C. Tengroth, U. Gasslander, F. O. Andersson, S. P. Jacobsson, *Pharm. Dev. Technol.* **2005**, 10, 405.
- [24] D. Kim, P. Tzeng, K. J. Barnett, Y. H. Yang, B. A. Wilhite, J. C. Grunlan, *Adv. Mater.* **2014**, 26, 746.
- [25] J. Li, Z. Jiang, H. Wu, L. Zhang, L. Long, Y. Jiang, *Soft Matter* **2010**, 6, 542.
- [26] Y. Matsumura, H. N. Ananthaswamy, *Toxicol. Appl. Pharmacol.* **2004**, 195, 298.
- [27] X. Wang, H. Chen, Y. Chen, M. Ma, K. Zhang, F. Li, Y. Zheng, D. Zeng, Q. Wang, J. Shi, *Adv. Mater.* **2012**, 24, 785.
- [28] Y. J. Wang, F. Caruso, *Chem. Mater.* **2005**, 17, 953.
- [29] T. A. Kolesnikova, D. A. Gorin, P. Fernandes, S. Kessel, G. B. Khomutov, A. Fery, D. G. Shchukin, H. Möhwald, *Adv. Funct. Mater.* **2010**, 20, 1189.
- [30] A. Z. Abbasi, L. a. Gutiérrez, L. L. del Mercato, F. Herranz, O. Chubykalo-Fesenko, S. Veintemillas-Verdaguer, W. J. Parak, M. P. Morales, J. s. M. González, A. Hernando, P. de la Presa, *J. Phys. Chem. C* **2011**, 115, 6257.
- [31] A. M. Pavlov, B. G. De Geest, B. Louage, L. Lybaert, S. De Koker, Z. Koudelka, A. Sapelkin, G. B. Sukhorukov, *Adv. Mater.* **2013**, 25, 6945.

- [32] D. G. Shchukin, G. B. Sukhorukov, H. Mohwald, *Angew. Chem. Int. Ed. Engl.* **2003**, *42*, 4472.
- [33] D. V. Volodkin, N. I. Larionova, G. B. Sukhorukov, *Biomacromolecules* **2004**, *5*, 1962.
- [34] A. A. Antipov, G. B. Sukhorukov, *Adv. Colloid Interface Sci.* **2004**, *111*, 49.
- [35] D. Usov, G. B. Sukhorukov, *Langmuir* **2010**, *26*, 12575.
- [36] G. S. Longo, M. Olvera de la Cruz, I. Szleifer, *Macromolecules* **2011**, *44*, 147.
- [37] J. C. Grunlan, L. Liu, O. Regev, *J. Colloid Interface Sci.* **2008**, *317*, 346.
- [38] M. Fertani-Gmati, M. Jemal, *J. Therm. Anal. Calorim.* **2015**, *123*, 757.
- [39] J. Park, Y. Han, H. Kim, *J. Nanomater.* **2012**, 528174.
- [40] S. A. Greenberg, *J. Phys. Chem.-Us* **1957**, *61*, 960.
- [41] Y. Niibori, M. Kunita, O. Tochiyama, T. Chida. *J. Nuclear Sci. Technol.* **2000**, *37*, 349.
- [42] H. R. Saghafi, A. Naderifar, S. Gerami, M. A. Emadi, *Can. J. Chem. Eng.* **2016**, *94*, 1880.
- [43] C. Ye, O. Shchepelina, R. Calabrese, I. Drachuk, D. L. Kaplan, V. V. Tsukruk, *Biomacromolecules* **2011**, *12*, 4319.

## Graphical abstract

